Research Square

Preprints are preliminary reports that have not undergone peer review.
They should not be considered conclusive, used to inform clinical practice,
or referenced by the media as validated information.

Toxicological Evaluation of Human Adipose-derived Mesenchymal Stem Cells (hADSCs) and hADSCs-derived Exosomes

Yang Zhou
Tongji University Affilliated East Hospital: Shanghai East Hospital https://orcid.org/0000-0002-6967-421X

Bo Zhao
Key Laboratory of Spine and Spinal Cord Injury Repair and Regeneration of Ministry of Education, Stem Cell Translational Research Center of Tongji Hospital, School of Life Science and Technology, Tongji University, 389 Xincun Road, Shanghai 200065, China

Xin-Liao Zhang
Tongji University School of Medicine

Yi-jun Lu
Tongji University School of Medicine

Jian Cheng
Tongji University School of Science and Technology

Yu Fu
Tongji University School of Science and Technology

Ning-Yan Zhang
Tongji University School of Science and Technology

Pei-Xin Li
Tongji University School of Medicine

Jing Zhang
Tongji University School of Science and Technology

Jun Zhang (junzhang@tongji.edu.cn)
Tongji University School of Medicine

Research Article

Keywords: Human adipose tissue-derived stem cells (hADSCs), Exosomes, Toxicology, Safety

Posted Date: June 30th, 2021

DOI: https://doi.org/10.21203/rs.3.rs-626854/v1

License: This work is licensed under a Creative Commons Attribution 4.0 International License.
Read Full License

Abstract

Background: Human adipose tissue-derived stem cells (hADSCs) are considered an ideal source of cells for regenerative medicine. Mesenchymal stem cells derived-exosomes (MSC-Exos) are being opined as new cell-free therapeutics for numerous human diseases. For future clinical applications, the safety of allogenic hADSCs and hADSCs-derived exosomes (hADSCs-Exos) needs to be addressed and verified in pre-clinical animal models. This study sought to evaluate the toxicity of hADSCs and hADSCs-Exos by performing *in vivo* and *in vitro* toxicological assessments.

Methods: We used IVIS to track the biodistribution of GFP-labeled hADSCs and the PKH26-labeled in a mouse model. The tumorigenicity of hADSCs and hADSCs-Exos was analyzed by soft agar colony formation assay and nude mice tumorigenicity test *in vitro* and *in vivo*. The acute animal toxicity and allergenicity test were used to explore the toxicological profile of hADSCs and hADSCs-Exos in mice.

Results: We found that hADSCs-Exos accumulated faster in the tissues of mice and were also cleared more rapidly compared to hADSCs. Both hADSCs and hADSCs-Exos have little risk of tumorigenicity, and hADSCs-Exos had lower toxicity and lower immunogenicity than hADSCs.

Conclusion: Our study is the first to compare the safety between hADSCs and hADSCs-Exos, and revealed that hADSCs-Exos are safer for application as systemic therapy, without complications in toxicological assessment, and have a better prospective utility as a treatment agent and for drug delivery.

Introduction

Mesenchymal stem cells (MSCs) have become a prospective cell treatment tool owing to their numerous properties, including multipotency, self-regenerating along with expansion ability, low immunogenicity, relatively simple to isolate from tissues, secretion of mediators that allow substitution or renovation of tissues [1, 2]. Human adipose-derived stem cells (hADSCs) are a stem cell population that originated from the SVF (stromal-vascular fractions) of the adipose tissue [3]. hADSCs have multiple differentiation potential and have also exhibited remarkable and reliable clinical utility value [4]. hADSC sources are ubiquitous, and isolation of hADSCs is secure, simple, and minimally invasive. For cell therapy, hADSCs have been proven to have immunosuppressive along with anti-inflammatory influences, as well as tissue repair and regeneration [4], which can be helpful to treat pathological wounds [5, 6], autoimmune disorders [7, 8], neurodegenerative diseases [9, 10], and other diseases [11, 12].

Paracrine cytokines, exosomes, and other active substances have been reported to be a major factor in which hADSCs exert their biological effects [13–15]. Numerous reports have documented that MSC transplantation therapy may work primarily through a paracrine mechanism where exosomes play a major role [16–19]. Recently, exosomes have gained attention as a promising alternative to conventional cell-based therapy. Exosomes are extracellular nano-scale vesicles, ranging between 30 and 200 nm in size, containing proteins and genetic material such as DNA, mRNA, and miRNA. They are transported to target cells for intercellular communication [20]. Exosomes offer improved safety and reliability

compared to parental cells without loss of function [21–23]. Therefore, exosomes have wide therapeutic potential in treating numerous diseases, for instance cancer [24], cardiovascular conditions [25], neurodegenerative diseases[26, 27], tissue damage [28, 29], as well as pathogenic infections [30].

There is a growing number of reports on the efficacy and roles of hADSCs and hADSCs-Exos. Despite the growing interest, the toxicity and safety researches of hADSCs and hADSCs-Eoxs are limited. Some studies have explored genotoxic, immunological, and hematological impacts of MSC-Exos, while some revealed the *in vitro* skin toxicity of hADSCs-Eoxs. The comprehension of the toxicity of hADSCs and hADSCs-Exos remains unclear. Herein, we first evaluated the non-clinical safety of hADSCs and hADSCs-Exos as drugs. We performed several toxicity tests to compare the differences between hADSCs and hADSCs-Exos in terms of *in vivo* biodistribution, *in vivo* tumorigenicity, *in vivo* acute animal toxicity, and *in vivo* allergenicity.

Materials And Methods

hADSCs Culture and hADSCs-GFP Construction

hADSCs were obtained from the Base of Stem Cell Translational Medicine of Shanghai East Hospital. hADSCs were processed, purified, and confirmed as described in our previous reports [31]. Briefly, hADSCs cells were cultured in a complete medium containing α-MEM (Gibco, USA) and 10% UltraGRO^{TM}-Advanced (Helios Bioscience, USA). After the cells attained confluence, they were digested with 0.25% trypsin-EDTA (Invitrogen), diluted 1:3, and plated for subculture. After 24 hours of cell attachment, the green fluorescent protein (GFP) Lentivirus (Genechem, Shanghai, China) infection was performed with an MOI of 100 as described by the manufacturer. After three passages, hADSCs stably expressing GFP were obtained, and hADSCs-GFP was successfully constructed.

Isolation and Identification of hADSCs-Exos

hADSCs-Exos were isolated, confirmed, and quantitated as described in our previous reports [31]. After reaching 80–90% confluence, hADSCs were rinsed in DPBS and incubated with a freshly prepared complete medium containing hADSCs-Exos-free FBS for two days. The culture supernatant was centrifuged at 300 *g* for 10 min to remove cells. The supernatant was transferred from the centrifugal tube to a new centrifugal tube and centrifuged at 2000 *g* for ten minutes. The cell debris was removed, and the supernatant was transferred to a new centrifugal tube again and centrifuged at 10,000 *g* for 30 minutes, then filtered through a 0.2-μm filter. Afterward, the supernatant was collected and centrifuged at 100,000 *g* for two hours at 4°C. After that, the supernatant was then discarded because the pellet contained hADSCs-Exos. hADSCs-Exos was re-suspended in 1×PBS and kept at − 80°C for subsequent experiments. A transmission electron microscope (TEM; FEI) was employed to explore the morphology of hADSCs-Exos. Besides, nanoparticle tracking analysis (NTA) was employed to determine the number along with the size of the isolated exosomes on a NanoSight NS300 system (NanoSight, Malvern, UK). The PKH26 red fluorescent cell linker kit (Sigma, St. Louis, MO, USA) was employed to label the hADSCs-Exos described by the manufacturer. The expressions of CD9, CD63, and CD81, which are exosome

surface biomarkers, were detected by western blot. Exosomes were lysed with RIPA lysis buffer (ThermoFisher, USA) enriched with the protease inhibitor cocktail and phosphatase inhibitor mini-tablets (Pierce, USA). The lysate was centrifuged at 3000 rpm for 15 minutes at 4°C. After that, the Micro Bicinchoninic Acid (BCA) Protein Assay Kit (Pierce) was used to quantify the proteins.

In Vivo **Imaging of Fluorescently labeled hADSCs and hADSCs-Exos**

For the *in vivo* bio-distribution analysis, a group of nude mice received GFP-labeled hADSCs (2×10^7 cells/kg of body weight) via a lateral tail vein. The mice were imaged using the In Vivo Imaging System Lumina K Series III (PerkinElmer, America) at diverse time points, 1, 2, 3, 4, 5, 7, 10, and 14 days post cell infusions. Then mice were sacrificed immediately after the *in vivo* imaging, and organs (heart, liver, spleen, lung, and kidney) were harvested. All fluorescence images were captured with 1s exposure times, and pseudo-color images indicating photon counts were analyzed using Living Image software (PerkinElmer, America).

For the *in vivo* bio-distribution studies of hADSCs-Exos, nude mice were infected with PKH26-labeled hADSCs-Exos (50 μg/kg of body weight) via the tail vein and imaged at 6, 12, 24, and 48 h after cell infusions with the Night Owl In Vivo Imaging System (LB 983, Berthold Technologies, Germany). Mice were sacrificed immediately after imaging, and organs (heart, liver, spleen, lung, and kidney) were harvested. All fluorescence images were captured and analyzed using IndiGo™ software (Berthold Technologies, Germany).

Soft agar colony formation assay

The ability of cells to grow anchorage independently was assessed with the soft agar colony formation assay. We conducted this assay according to previous angiosarcoma studies [32]. Concisely, 4 ml of 0.6% low-melting agarose (Sigma-Aldrich, St. Louis, MO) dispersed in DMEM enriched 10% FBS was poured into a 60 mm culture plate and left to form a bottom layer of agar. Afterward, 2 ml of 0.7% low-melting agarose containing 5×10^4 hADSCs dispersed in α-MEM enriched with 10% UltraGRO^{TM}-Advanced (Helios Bioscience, USA) was poured on top of the bottom layer and left to form the top layer. The dishes were incubated at 37°C and 5% CO_2 conditions and monitored daily. A microscope was employed to observe and image the cells on day 14.

Nude Mice Tumorigenicity Test

Overall, 144 nude mice, half male and half female, were commercially acquired from Shanghai Slake Laboratory Animal Co. Ltd. (Shanghai, China). The experiment was initiated with 6-week-old mice weighing 20–25 g. The nude mice were randomly divided into four groups, with 36 animals (18 males and 18 females) in each group. The negative control group received normal saline, the hADSCs groups received 2×10^7 cells/kg hADSCs, the hADSCs-Exos groups received 50 μg/kg exosomes, and the positive control group received 2×10^7 cells/kg Hela cells in 100 μL of normal saline intranasally. Subcutaneous injections were given into the right axilla of each nude mouse. The animals were observed and weighed

once a week after administering the solutions during the testing period for all animals. We measured the sizes of the visible nodules using a vernier caliper and recorded the values every seven days. All mice were sacrificed at 2 months after the injection, with an overdose of anesthesia solution by intraperitoneal injection. The heart, liver, kidney, lung, and spleen were removed and weighed. The wet-weight index (%) was calculated as follows: (organ wet-weight/body weight) × 100%. Sections of major organs were prepared and stained with hematoxylin-eosin (H&E) for histopathological assays.

Acute Toxicity Test in Mice

Six-week-old C57BL/6 mice were purchased from Shanghai Slake Laboratory Animal Co. Ltd. All animals were divided into five groups with 20 mice per group (10 males and 10 females): negative control group (normal saline), hADSCs high-dose group (2×10^8 cells/kg), hADSCs low-dose group (2×10^7 cells/kg), hADSCs-Exos high-dose group (500 μg/kg), and hADSCs-Exos low-dose group (50 μg/kg). All compounds were administered by lateral tail vein injection in a 100-μl volume (5 mL/kg) and were completed within one minute. After dosing, toxic signs and mortalities were observed and documented continuously for 14 days. The body weights of all the animals were recorded every three days. After the experiment, the animals were sacrificed, organs were harvested, and the wet-weight index was measured. Every animal found dead or euthanized was immediately subjected to necropsy.

Guinea Pig Active Systemic Allergy Test

Guinea pigs of either sex weighing 250–300 g were randomized into six groups of 12 animals (half female and half male). Respectively, hADSCs at a high-dose of 2×10^8 cells/kg and a low-dose of 2×10^7 cells/kg, hADSCs-Exos at a high-dose of 500 μg/kg and a low-dose of 50 μg/kg, normal saline, or bovine serum albumin (BSA) of 20 mg/kg in 1 ml were subcutaneously administered by intraperitoneal injection into guinea pigs for immuno-sensitization, every other day, for three times. At day 19 post-initial injection, the sensitizers described above were inoculated intraperitoneally with double the sensitizing dose. After that, allergic response symptoms, manifested as involuntary urination, frequent nose scratching, shivering, dyspnea, piloerection, convulsive spasms, shock, or even death, were observed [33]. Classification criteria for sensitization were [34]: symptoms of convulsive spasms, involuntary urination, dyspnea, shock, or death (++++); symptoms of frequent coughs, consisting of convulsive spasms, dyspnea (+++); symptoms of a few coughs, with nose scratching, piloerection, or shivering, (++); slight symptoms of nose scratching, piloerection, or shivering, (+); and non-reactive (−).

Histological analysis

Tissues were harvested from mice and fixed in 4% PFA overnight, then dehydrated and embedded in paraffin, and finally sliced into 4-μm thick coronal sections by a microtome. For H&E staining, the sections were stained with hematoxylin and rinsed in water. After that, they were stained with eosin, dehydrated, and lastly mounted.

Statistical analyses

Statistical analyses were implemented in the GraphPad Prism software. Two-tailed Student's *t*-test was implemented when there were only two groups of samples, while one-way ANOVA was used in comparing more than two groups of samples and two-way ANOVA for more than two conditions. ANOVA analysis was followed by *post hoc* Bonferroni's correction for multiple comparisons. $P < 0.05$ signified statistical significance; *p-value < 0.05, **p-value < 0.01, ***p-value < 0.001, ****p-value < 0.0001. The data exhibited a normal distribution. The estimated variance was similar between experimental groups. Data are given as the mean ± SD or ± SEM as illustrated in the figure legends.

Results

Biodistribution of hADSCs and hADSCs-Exos

The fluorescence images and white light images taken by the microscope of hADSCs-GFP were displayed in Fig. 1A, B. The transfection rate of hADSCs was almost 90%, with stable GFP expression after subculture. GFP-labeled hADSCs were injected into nude mice via the tail vein. To explore the biodistribution, we employ an *in vivo* imaging system (IVIS) to image live mice at different time points after inoculation with GFP-labeled hADSCs (Fig. 1C). As indicated in these representative photographs, the levels of detail from fluorescent imaging of the whole mouse did not warrant adequate accuracy to conclude from which tissue the signal originates. Therefore, to determine the organ from which the fluorescent signal originated and minimize interference of signals, we harvested the organs and imaged them ex vivo in subsequent experiments. So, the mice were sacrificed and organs excised at the corresponding different time points. Twenty-four hours after intravenous injection, most hADSCs appeared to have aggregated in the lung, liver, and kidney. Fluorescent levels peaked 48 h after hADSCs-GFP intravenous injection and tapered gradually throughout seven days. Signals were detected up to 10 days post cell infusion but not after that.

hADSCs-Exos were isolated from hADSCs supernatants by ultracentrifugation. The exosome particle sizes and concentrations were measured via nanoparticle tracking analysis (NTA), and diameters were approximately 30–200 nm (Fig. 1D). The hADSCs-Exos pellets were examined by TEM, and spherical vesicles were visible, as shown in Fig. 1E. The expression of widely expressed exosome surface markers, such as the CD9, CD81, and CD63, was verified by western blotting (Fig. 1F). PKH26 is a lipophilic membrane dye and is being used increasingly in studies of exosomes and their functions. PKH dyes, including PKH26, are recognized to have an *in vivo* half-life ranging from 5 to > 100 days. The fluorescence signal of pHK26 can well reflect the biodistribution and metabolism of exosomes *in vivo*. Nude mice intravenously injected with PKH26 labeled hADSCs-Exos were imaged using an IVIS 200 Optical Imaging System at 6, 12, 24, and 48 hours post-injection. At these four different time points, the mice were sacrificed and the organs excised. Six hours after intravenous injection, hADSCs-Exos were primarily accumulated in the lung, liver, and kidney. The highest hADSCs-Exos signal was detected at 12 hours post-injection, and the fluorescent finally disappeared at about 48 h (Fig. 1G). These results indicate that hADSCs and hADSCs-Exos have similar distribution patterns, and they both have a higher accumulation in the lung than in other tissues. Notably, whereas the hADSCs-Exos signal disappeared at

48 hours in the lung, liver, and kidney, hADSCs showed the most signal in these organs. Overall, these results indicated that hADSCs-Exos accumulated faster in the lung, liver, and kidney and were also cleared more rapidly than hADSCs.

Tumorigenicity of hADSCs and hADSCs-Exos

hADSC cells' rapid growth rate raised the possibility that they were tumorigenically transformed, and two standard approaches in our study explored this. Firstly, the soft agar colony formation assay illustrated that hADSC cells could proliferate and did not form large colonies in an anchorage-independent manner (Fig. 2A). Secondly, a tumorigenicity test was performed to assess the safety of hADSCs and hADSCs-Exos. Nude mice were injected with hADSCs, hADSCs-Exos, Hela cells, or physiological saline in the right armpit. Hela cells were used as positive controls. The mice were observed for tumor formation weekly and photographed at the end of two months. Nodules were observed in female and male mice in the Hela cells group at day 63, reaching a maximum of 366 mm^2 in male mice and 319 mm^2 in female mice (Fig. 2B). Nevertheless, likewise to the physiological saline control group, subcutaneous nodules were not visible in the male and female mice of the hADSCs and hADSCs-Exos group. Mice were sacrificed and necropsied to collect the significant organs for histopathological analyses at 63 days after administration. No remarkable intergroup differences were detected in mice's body weight (Fig. 2C). In addition, no abnormalities were found in organ weight and pathological assessment of the organs in the hADSCs group and hADSCs-Exos group, compared with the Hela cells groups (Fig. 2D, E). These results demonstrated that both hADSCs and hADSCs-Exos have little risk of tumorigenicity.

Acute Toxicity Studies of hADSCs and hADSCs-Exos

All animals tolerated the intravenous hADSCs and hADSCs-Exos infusion with two doses, respectively. The high dose of hADSCs is 5×10^6 cells/mouse (equal to 2×10^8 cell/kg), and the low dose is 5×10^5 cells/mouse (equal to 2×10^7 cell/kg). Regarding hADSCs-Exos dosage, 10ug/mouse (equal to 500ug/kg) is the high dose, and 1ug/mouse (equal to 50ug/kg) is low. In the hADSCs high-dose group, 30 minutes after administration, six female and three male healthy mice showed convulsions, tachycardia, unresponsiveness, dilated pupils, and finally death. It appears that the issue could be due to transient lung emboli [35]. The remaining 11 mice (4 females and 7 males) in hADSCs high-dose group had some immediate side events symptoms, including restless, dyspnea, and reduced activity, which resolved within 24 h. These above symptoms were not observed in the control group or hADSCs low-dose or hADSCs-Exos high- and low-dose groups. At 14 days after administration, we sacrificed all the animals and collected the major organs for evaluating the *in vivo* toxicology by histological examination. As shown in Fig. 3A, there were no significant differences in mice's body weights from all groups. Viscera percentage assessment of the tissue follow-up did not reveal any obvious abnormality linked to cell infusion (Fig. 3B).

Active Systemic Anaphylaxis Test of hADSCs and hADSCs-Exos

As shown in various publications, false-positive stimulation indices due to irritation may be obtained in the mouse model [36]. To provide the basis for the clinical trial and clinical application, we evaluated the allergic reaction of guinea pigs to hADSCs and hADSCs-Exos. The active systemic anaphylaxis test was designed in Fig. 4. No abnormalities were found in the appearance, behavior, secretion, and excreta of guinea pigs during the quarantine and sensitization phases. There was no remarkable difference in the weight of guinea pigs at each time point and each dose group in contrast with the negative control group. On day 19, guinea pigs were monitored for allergic reactions within 2 h post-challenge, and then the allergic reaction symptoms were evaluated.

In comparison to the negative control, nine were strongly positive (+++), and three were positive (++) in the positive control group. In the hADSCs high-dose group, 1 sample was positive (+), three samples were weakly positive (++), eight samples were negative (–). In the hADSCs low-dose group, only one weakly positive (+) sample was observed. No animals in the hADSCs-Exos high- and low-dose groups or in the negative control group had any obvious allergic reaction after the challenge. Animal death was not observed. Overall, hADSCs-Exos had lower immunogenicity compared to hADSCs (Table 1).

Table 1
Levels on symptoms of active systemic anaphylaxis of guinea pig in various groups

Group	N	Level of allergic reaction symptoms					Incidence of positive reaction	Incidence of extremely strong positive reaction
		-	+	++	+++	++++		
negative control	12	12	0	0	0	0	0%	0%
positive control	12	0	0	3	9	0	100%	0%
hADSCs high-dose	12	8	3	1	0	0	33%	0%
hADSCs low-dose	12	11	1	0	0	0	8%	0%
hADSCs-Exo high-dose	12	12	0	0	0	0	0%	0%
hADSCs-Exo low-dose	12	12	0	0	0	0	0%	0%

Discussion

Herein, we explored the safety and toxicology of hADSCs and hADSCs-Exos as the prelude to their future utilization as treatment agents. Although the biological and functional roles of hADSCs and hADSCs-Exos are extensively investigated, there is a dearth of information concerning the toxicological aspects of using them. Therefore, characterization of the safety and toxicity of hADSCs and hADSCs-Exos is

essential before their use in clinical trials. In this study, we first evaluated the non-clinical safety and toxicity of hADSC and hADSCs-Exos. We compared the differences between them in biodistribution, tumorigenicity, acute animal toxicity, and allergenicity. Our current findings contribute significantly to our understanding of the safety of hADSCs and hADSCs-Exos in several ways and provide a basis for the clinical application of hADSCs and their secreted exosomes.

First, we examined the biodistribution of fluorescently-labeled hADSCs and hADSCs-Exos using an IVIS. We found that they were both mainly distributed in the lungs, liver, and kidneys after intravenous injection. The fluorescent signal of hADSCs reached the peak at 48h and was detected up to 14 days after cell infusion, while hADSCs-Exos' fluorescent showed the strongest signal at 24h and disappeared at 48h. These data indicated that hADSCs-Exos accumulated faster in these tissues and cleared more rapidly than hADSCs. Our data are consistent with previous studies on the biodistribution of MSC and MSC-Exo [37]. In addition, hADSC cells, like other cells, first move to the lung following i.v. infusion [38]. These results are validated in mice in the present study, in which homing to the lungs is reported up to several days after i.v. infusion. Studies should be designed to explore the possible hADSCs triggered side-events in the lungs, for instance, thrombosis or pneumonia. No pulmonary embolism was reported in this study.

Tumorigenicity analysis using nude mice administered hADSCs and hADSCs-Exos revealed no formation of subcutaneous nodules, suggesting that there is no serious risk of tumor development. Besides, there were no abnormal results, such as tumor development in systemic organs, indicating no severe risk of toxicity. More precisely, hADSC cells could proliferate and did not form large colonies in an anchorage-independent manner. What's more, in our study, treating animals with doses up to 2×10^8/kg (high dose), we see some healthy mice died of pulmonary embolism. Some other hADSCs high- and low-dose treated mice had some immediate side effects symptoms, but which resolved within 24 h. In hADSCs-Exos high- and low-dose groups, we did not see any side effects symptoms. This result verifies that even extremely high doses of hADSCs-Exos seem safe as per the clinical safety reports using doses around 500ug/kg. The histology of all evaluated organs did not reveal any adverse events by infusion of hADSCs and hADSCs-Exos. Concerning allergenicity, hADSCs-Exos had lower immunogenicity.

Apart from the toxicological studies discussed above, the administered dose of hADSCs and hADSCs-Exos is crucial. Due to the complexity of the content of MSCs and their exosomes [37], different administered doses produce different toxicity effects, and the doses differ considerably among different studies[39–41]. Our research indicated that the hADSCs at a low dose (2×10^7 cells/kg) used in this study are much safer compared to the significant toxicity of a higher dose (2×10^8 cells/kg) in our animal model. In addition, the protein composition and their immunomodulatory functions are considered a cause of immune responses after administration. Some researchers have shown that exosomes have immune evasion properties [42]. Although the mechanism responsible for immune evasion of exosomes remains unclear, we also found lower immunogenicity of exosomes in this study.

Conclusion

In the present study, we explored the biodistribution, toxicological profile, and immunogenic potential of hADSCs and hADSCs-Exos. We established that the hADSCs-Exos are safe with no complications because hADSCs-Exos had lower toxicity and lower immunogenicity than hADSCs at the corresponding administered doses, and neither showed signs of tumorigenicity. Although MSC-originated exosomes have been documented in pre-clinical studies as secure, their complex structure, the alterable composition, as well as oncogenic along with immunogenic ability, might impede their clinical utility. A promising option involved developing exosome mimics to improve their uptake, stability, targeting, and immunogenicity. More studies should be conducted on the standard and promising strategies concerning manufacturing exosomes at a large scale under GMP and the storage conditions required to transfer exosomes to clinical utility.

Abbreviations

hADSC: human adipose-derived mesenchymal stem cells; hADSC-Exo: human adipose-derived mesenchymal stem cells derived exosomes; TEM: Transmission electron microscopy; NTA: Nanosight tracking analysis; PBS: Phosphate-buffered saline; SEM: Scanning electron microscopy; IVIS In Vivo Imaging System.

Declarations

Acknowledgments

We thank the Translational Medical Center for Stem Cell Therapy of Shanghai East Hospital for their assistance and guidance for hADSCs culture.

Authors' contributions

YZ conceived the idea for the project, designed all experiments, and analyzed data. BZ performed major experiments and analyzed data. XLZ, YJL, JC, YF, NYZ, and PXL assisted in performing experiments. YZ and BZ wrote the manuscript. JZ and JZ verified the final version of the manuscript. All authors read and approved the final manuscript.

Funding

This research project was supported by the National Natural Science Foundation of China (81771417, 31371379 and 31271120), the National Key Research and Development Program of China [2016YFA0700800], Major Program of Development Fund for Shanghai Zhangjiang National Innovation Demonstration Zone <Stem Cell Strategic Biobank and Stem Cell Clinical Technology Transformation Platform> [ZJ2018-ZD-004], the Peak Disciplines (Type IV) of Institutions of Higher Learning in Shanghai.

Availability of data and materials

Data and reagents will be provided upon availability and reasonable request.

Ethics approval and consent to participate

All human samples and animal studies were approved by the Committee of Ethics on Experimentation of Tongji University. The experiments were conducted following the National Institutes of Health guidelines for the care and use of animals.

Consent for publication

Not applicable.

Competing interests

The authors declare that they have no competing interests.

References

1. Rajabzadeh N., Fathi E., Farahzadi R. Stem cell-based regenerative medicine, Stem Cell Investig 2019: 6: 19.
2. Uccelli A., Moretta L., Pistoia V. Mesenchymal stem cells in health and disease, Nature reviews Immunology 2008: 8: 726-736.
3. Mahmoudifar N., Doran P. M. Mesenchymal Stem Cells Derived from Human Adipose Tissue, Methods in molecular biology (Clifton, NJ) 2015: 1340: 53-64.
4. Shukla L., Yuan Y., Shayan R. et al. Fat Therapeutics: The Clinical Capacity of Adipose-Derived Stem Cells and Exosomes for Human Disease and Tissue Regeneration, Front Pharmacol 2020: 11: 158.
5. Ahmadi A. R., Chicco M., Huang J. et al. Stem cells in burn wound healing: A systematic review of the literature, Burns : journal of the International Society for Burn Injuries 2019: 45: 1014-1023.
6. Goodarzi P., Alavi-Moghadam S., Sarvari M. et al. Adipose Tissue-Derived Stromal Cells for Wound Healing, Adv Exp Med Biol 2018: 1119: 133-149.
7. Kokai L. E., Marra K., Rubin J. P. Adipose stem cells: biology and clinical applications for tissue repair and regeneration, Translational research : the journal of laboratory and clinical medicine 2014: 163: 399-408.
8. Wainstein C., Quera R., Fluxá D. et al. Stem Cell Therapy in Refractory Perineal Crohn's Disease: Long-term Follow-up, Colorectal disease : the official journal of the Association of Coloproctology of Great Britain and Ireland 2018.
9. Zhang P., Tian B. Metabolic syndrome: an important risk factor for Parkinson's disease, Oxidative medicine and cellular longevity 2014: 2014: 729194.
10. Yan Y., Ma T., Gong K. et al. Adipose-derived mesenchymal stem cell transplantation promotes adult neurogenesis in the brains of Alzheimer's disease mice, Neural Regen Res 2014: 9: 798-805.
11. Fang Y., Tian X., Bai S. et al. Autologous transplantation of adipose-derived mesenchymal stem cells ameliorates streptozotocin-induced diabetic nephropathy in rats by inhibiting oxidative stress, pro-

inflammatory cytokines and the p38 MAPK signaling pathway, Int J Mol Med 2012: 30: 85-92.

12. Richardson S. M., Kalamegam G., Pushparaj P. N. et al. Mesenchymal stem cells in regenerative medicine: Focus on articular cartilage and intervertebral disc regeneration, Methods (San Diego, Calif) 2016: 99: 69-80.
13. L. P. K., Kandoi S., Misra R. et al. The mesenchymal stem cell secretome: A new paradigm towards cell-free therapeutic mode in regenerative medicine, Cytokine & Growth Factor Reviews 2019.
14. Liang X., Ding Y., Zhang Y. et al. Paracrine mechanisms of mesenchymal stem cell-based therapy: current status and perspectives, Cell Transplant 2014: 23: 1045-1059.
15. Song M., Heo J., Chun J. Y. et al. The paracrine effects of mesenchymal stem cells stimulate the regeneration capacity of endogenous stem cells in the repair of a bladder-outlet-obstruction-induced overactive bladder, Stem cells and development 2014: 23: 654-663.
16. Hu P., Yang Q., Wang Q. et al. Mesenchymal stromal cells-exosomes: a promising cell-free therapeutic tool for wound healing and cutaneous regeneration, Burns Trauma 2019: 7: 38.
17. Qiu G., Zheng G., Ge M. et al. Functional proteins of mesenchymal stem cell-derived extracellular vesicles, Stem cell research & therapy 2019: 10: 359.
18. Zhang S., Teo K. Y. W., Chuah S. J. et al. MSC exosomes alleviate temporomandibular joint osteoarthritis by attenuating inflammation and restoring matrix homeostasis, Biomaterials 2019: 200: 35-47.
19. Ling L., Feng X., Wei T. et al. Human amnion-derived mesenchymal stem cell (hAD-MSC) transplantation improves ovarian function in rats with premature ovarian insufficiency (POI) at least partly through a paracrine mechanism, Stem cell research & therapy 2019: 10: 46.
20. Rong X., Greening D. W., Zhu H. J. et al. Extracellular vesicle isolation and characterization: toward clinical application, Journal of Clinical Investigation 2016: 126: 1152-1162.
21. Rani S., Ryan A. E., Griffin M. D. et al. Mesenchymal Stem Cell-derived Extracellular Vesicles: Toward Cell-free Therapeutic Applications, Molecular therapy : the journal of the American Society of Gene Therapy 2015: 23: 812-823.
22. Das C. K., Jena B. C., Banerjee I. et al. Exosome as a Novel Shuttle for Delivery of Therapeutics across Biological Barriers, Molecular pharmaceutics 2019: 16: 24-40.
23. Burger D., Vinas J. L., Akbari S. et al. Human endothelial colony-forming cells protect against acute kidney injury: role of exosomes, Am J Pathol 2015: 185: 2309-2323.
24. Munson P., Shukla A. Exosomes: Potential in Cancer Diagnosis and Therapy, Medicines (Basel, Switzerland) 2015: 2: 310-327.
25. Khan M., Nickoloff E., Abramova T. et al. Embryonic stem cell-derived exosomes promote endogenous repair mechanisms and enhance cardiac function following myocardial infarction, Circulation research 2015: 117: 52-64.
26. Dinkins M. B., Dasgupta S., Wang G. et al. Exosome reduction in vivo is associated with lower amyloid plaque load in the 5XFAD mouse model of Alzheimer's disease, Neurobiol Aging 2014: 35:

1792-1800.
27. Hill A. F. Extracellular Vesicles and Neurodegenerative Diseases, J Neurosci 2019: 39: 9269-9273.
28. Tan C. Y., Lai R. C., Wong W. et al. Mesenchymal stem cell-derived exosomes promote hepatic regeneration in drug-induced liver injury models, Stem cell research & therapy 2014: 5: 76.
29. Mitchell R., Mellows B., Sheard J. et al. Secretome of adipose-derived mesenchymal stem cells promotes skeletal muscle regeneration through synergistic action of extracellular vesicle cargo and soluble proteins, Stem cell research & therapy 2019: 10: 116.
30. Li J., Liu K., Liu Y. et al. Exosomes mediate the cell-to-cell transmission of IFN-α-induced antiviral activity, Nature immunology 2013: 14: 793-803.
31. Zhou Y., Zhao B., Zhang X. L., et al. Combined topical and systemic administration with human adipose-derived mesenchymal stem cells (hADSC) and hADSC-derived exosomes markedly promoted cutaneous wound healing and regeneration, Stem cell research & therapy 2021: 12: 257.
32. Ning H., Liu G., Lin G. et al. Identification of an aberrant cell line among human adipose tissue-derived stem cell isolates, Differentiation 2009: 77: 172-180.
33. Antonisamy P., Ignacimuthu S. Immunomodulatory, analgesic and antipyretic effects of violacein isolated from Chromobacterium violaceum, Phytomedicine : international journal of phytotherapy and phytopharmacology 2010: 17: 300-304.
34. Meng Y., Liu B., Lei N. et al. Alpha-momorcharin possessing high immunogenicity, immunotoxicity and hepatotoxicity in SD rats, Journal of ethnopharmacology 2012: 139: 590-598.
35. Sadeghi B., Moretti G., Arnberg F. et al. Preclinical Toxicity Evaluation of Clinical Grade Placenta-Derived Decidua Stromal Cells, Front Immunol 2019: 10: 2685.
36. Maurer T. Guinea pigs in hypersensitivity testing, Methods (San Diego, Calif) 2007: 41: 48-53.
37. Wiklander O. P., Nordin J. Z., O'Loughlin A. et al. Extracellular vesicle in vivo biodistribution is determined by cell source, route of administration and targeting, Journal of extracellular vesicles 2015: 4: 26316.
38. Vilalta M., Degano I. R., Bago J. et al. Biodistribution, long-term survival, and safety of human adipose tissue-derived mesenchymal stem cells transplanted in nude mice by high sensitivity non-invasive bioluminescence imaging, Stem cells and development 2008: 17: 993-1003.
39. Takahashi Y., Nishikawa M., Shinotsuka H. et al. Visualization and in vivo tracking of the exosomes of murine melanoma B16-BL6 cells in mice after intravenous injection, Journal of biotechnology 2013: 165: 77-84.
40. Alvarez-Erviti L., Seow Y., Yin H. et al. Delivery of siRNA to the mouse brain by systemic injection of targeted exosomes, Nature biotechnology 2011: 29: 341-345.
41. Zhang S., Danchuk S. D., Imhof K. M. et al. Comparison of the therapeutic effects of human and mouse adipose-derived stem cells in a murine model of lipopolysaccharide-induced acute lung injury, Stem cell research & therapy 2013: 4: 13.

42. Kusuma R. J., Manca S., Friemel T. et al. Human vascular endothelial cells transport foreign exosomes from cow's milk by endocytosis, American journal of physiology Cell physiology 2016: 310: C800-807.

Figures

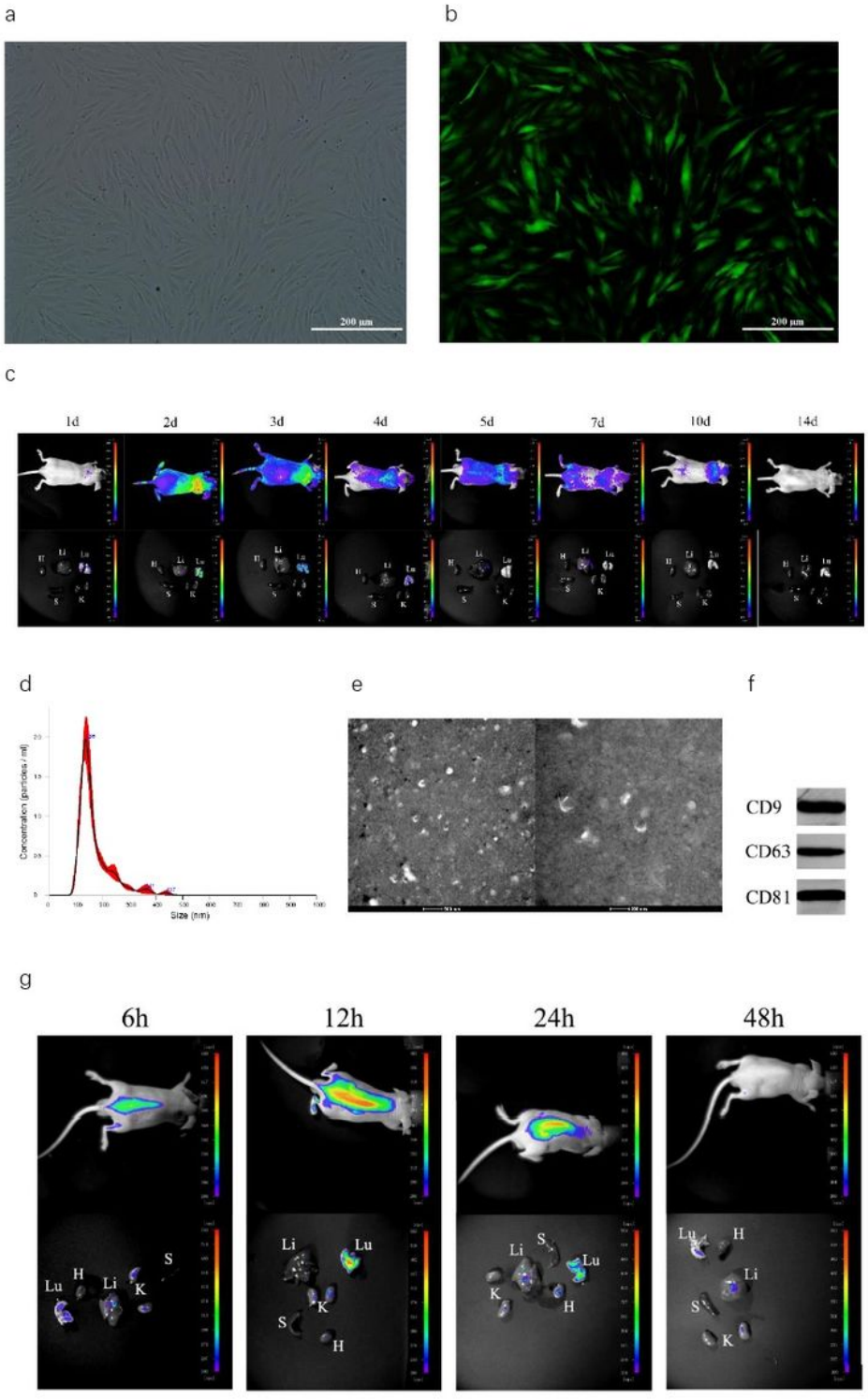

Figure 1

In vivo hADSCs and hADSCs-Exos biodistribution. a hADSCs were in fibroblast-like shape. b Fluorescence images of GFP-infected hADSCs. Scale bars = 100 μm. c IVIS images of the mice and their organs from 1 d to 14 d after receiving an intravenous injection of GFP-hADSCs. d The size of hADSCs-Exos were analyzed with NTA. e hADSCs-Exos morphology viewed by TEM. Bars represent 500 nm and 200 nm. f Exosome surface markers CD9, CD63, CD81 were detected by western blotting. g IVIS images of the mice and their organs from 6 h to 48 h after receiving an intravenous injection of PKH26-hADSCs-Exos. H, heart; Lu, lung; Li, liver; S, spleen; K, kidney.

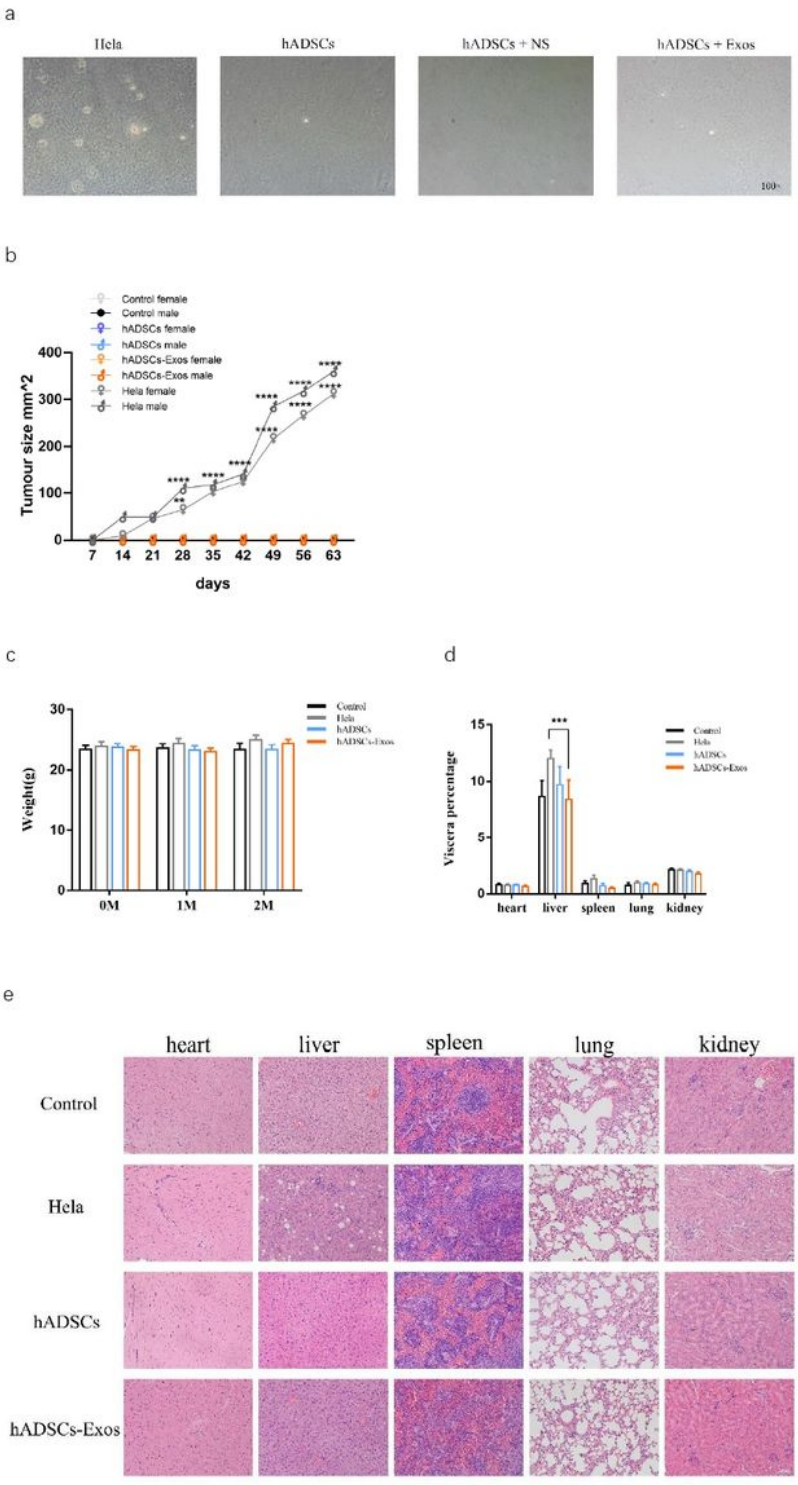

Figure 2

Tumorigenicity test of hADSCs and hADSCs-Exos. a hADSCs and hADSCs-Exos were explored for the potential to grow anchorage independently. Hela cells were used as a positive control. Magnification, 100×. b Mean tumor volumes were calculated every seven days. n = 6. c Bodyweights of nude mice in each group. Data are given as means ± SD (n = 12; half male and half female). d Viscera percentage = viscera weight / bodyweight (n = 6). e H&E staining of the heart, liver, spleen, lung, and kidney after two months. Scale bar = 100 μm. Results are presented as mean ± standard error of the mean; n = 36 for each group (18 males and 18 females). *p-value < 0.05, **p-value < 0.01, ***p-value < 0.001 vs vehicle control group.

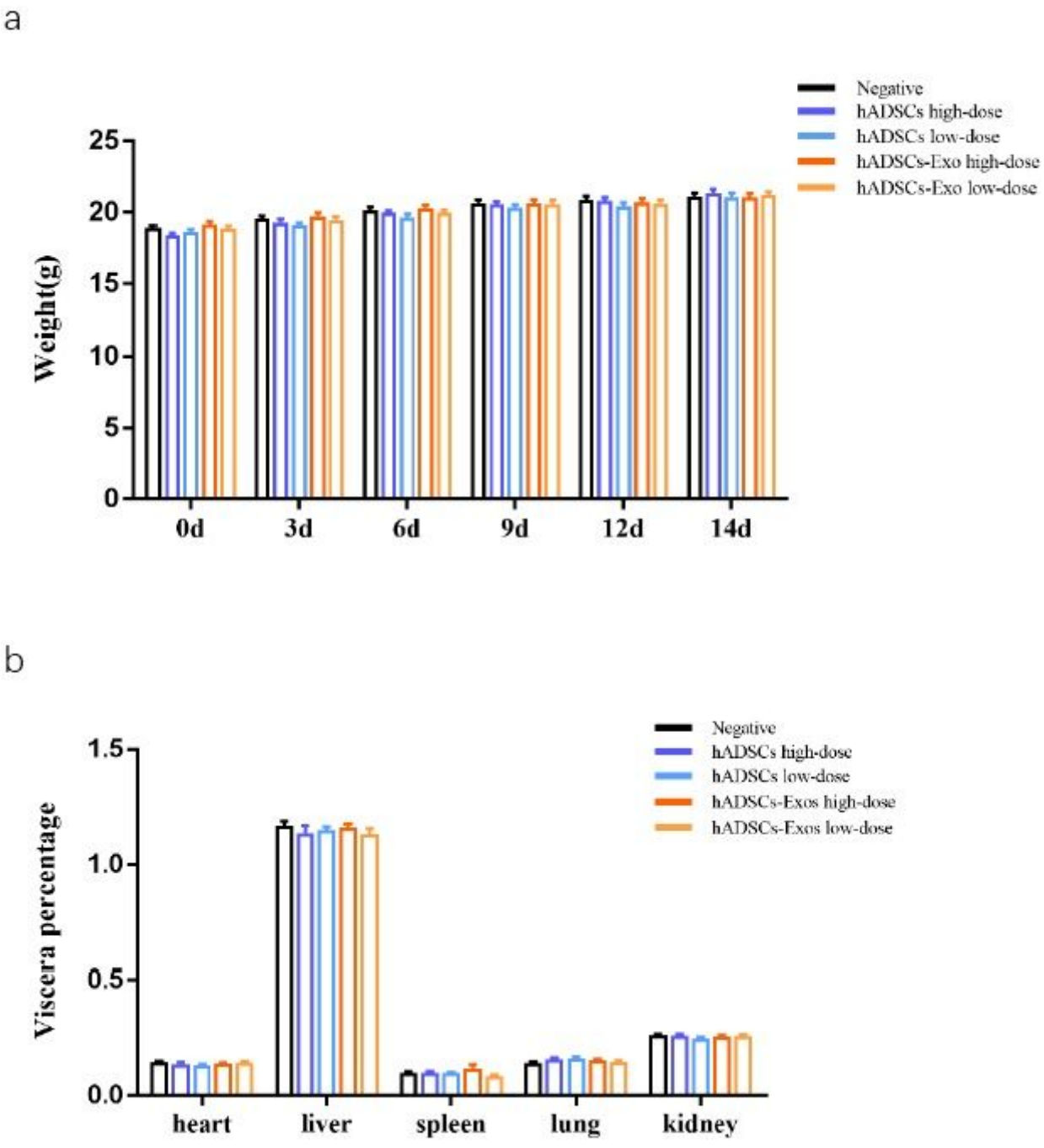

Figure 3

Toxicity test of hADSCs and hADSCs-Exos. a Bodyweights of the C57BL/6 mice in the single-dose toxicity test. Data are expressed as means ± SD (n = 20; half male and half female). b Viscera percentage = viscera weight/bodyweight on day 14. Results are presented as mean ± standard error of the mean; n = 20 for each group (10 males and 10 females). *p-value < 0.05, **p-value < 0.01, ***p-value < 0.001 vs vehicle control group.

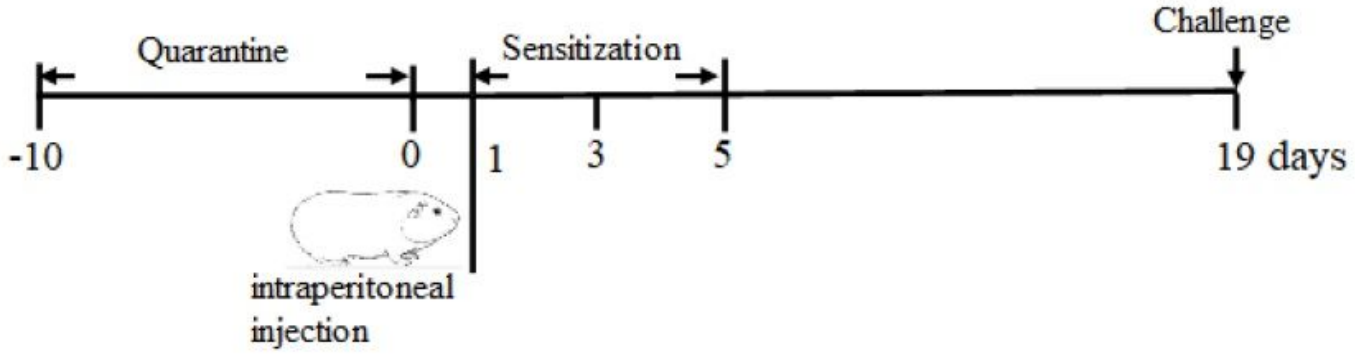

Figure 4

Sensitization protocol for guinea pigs After a 10-day quarantine period, guinea pigs were sensitized on days 1, 3, and 5 with the sensitizing dose via intraperitoneal injection and were challenged twice 19th day after the last sensitization. n = 12 for each group (6 males and 6 females).